

AN EXCEPTIONAL VERY HIGH ENERGY GAMMA-RAY FLARE OF PKS 2155–304

F. AHARONIAN,^{1,2,3} A. G. AKHPERJANIAN,⁴ A. R. BAZER-BACHI,⁵ B. BEHERA,⁶ M. BEILICKE,⁷ W. BENBOW,² D. BERGE,^{2,8} K. BERNLÖHR,^{2,9} C. BOISSON,¹⁰ O. BOLZ,² V. BORREL,⁵ T. BOUTELIER,¹¹ I. BRAUN,² E. BRION,¹² A. M. BROWN,¹³ R. BÜHLER,² I. BÜSCHING,¹⁴ T. BULIK,¹⁵ S. CARRIGAN,² P. M. CHADWICK,¹³ A. C. CLAPSON,² L.-M. CHOUNET,¹⁶ G. COIGNET,¹⁷ R. CORNILS,⁷ L. COSTAMANTE,^{2,18} B. DEGRANGE,¹⁶ H. J. DICKINSON,¹³ A. DJANNATI-ATAÏ,¹⁹ W. DOMAINKO,² L. O’C. DRURY,³ G. DUBUS,¹⁶ J. DYKS,¹⁵ K. EGBERTS,² D. EMMANOULOPOULOS,⁶ P. ESPIGAT,¹⁹ C. FARNIER,²⁰ F. FEINSTEIN,²⁰ A. FIASSON,²⁰ A. FÖRSTER,² G. FONTAINE,¹⁶ SEB. FUNK,⁹ S. FUNK,² M. FÜBLING,⁹ Y. A. GALLANT,²⁰ B. GIEBELS,¹⁶ J. F. GLICENSTEIN,¹² B. GLÜCK,²¹ P. GORET,¹² C. HADJICHRISTIDIS,¹³ D. HAUSER,² M. HAUSER,⁶ G. HEINZELMANN,⁷ G. HENRI,¹¹ G. HERMANN,² J. A. HINTON,^{2,6,22} A. HOFFMANN,²³ W. HOFMANN,² M. HOLLERAN,¹⁴ S. HOPPE,² D. HORNS,²³ A. JACHOLKOWSKA,²⁰ O. C. DE JAGER,¹⁴ E. KENDZIORRA,²³ M. KERSCHHAGGL,⁹ B. KHÉLIFI,^{2,16} NU. KOMIN,²⁰ K. KOSACK,² G. LAMANNA,¹⁷ I. J. LATHAM,¹³ R. LE GALLOU,¹³ A. LEMIERE,¹⁹ M. LEMOINE-GOUMARD,¹⁶ J.-P. LENAIN,¹⁰ T. LOHSE,⁹ J. M. MARTIN,¹⁰ O. MARTINEAU-HUYNH,²⁴ A. MARCOWITH,²⁰ C. MASTERSON,³ G. MAURIN,¹⁹ T. J. L. MCCOMB,¹³ R. MODERSKI,¹⁵ E. MOULIN,^{12,20} M. DE NAUROS,²⁴ D. NEDBAL,²⁵ S. J. NOLAN,¹³ J.-P. OLIVE,⁵ K. J. ORFORD,¹³ J. L. OSBORNE,¹³ M. OSTROWSKI,²⁶ M. PANTER,² G. PEDALETTI,⁶ G. PELLETIER,¹¹ P.-O. PETRUCCI,¹¹ S. PITA,¹⁹ G. PÜHLHOFER,⁶ M. PUNCH,¹⁹ S. RANCON,¹⁷ B. C. RAUBENHEIMER,¹⁴ M. RAUE,⁷ S. M. RAYNER,¹³ M. RENAUD,² J. RIPKEN,⁷ L. ROB,²⁵ L. ROLLAND,¹² S. ROSIER-LEES,¹⁷ G. ROWELL,^{2,27} B. RUDAK,¹⁵ J. RUPPEL,²⁸ V. SAHAKIAN,⁴ A. SANTANGELO,²³ L. SAUGÉ,¹¹ S. SCHLENKER,⁹ R. SCHLICKEISER,²⁸ R. SCHRÖDER,²⁸ U. SCHWANKE,⁹ S. SCHWARZBURG,²³ S. SCHWEMMER,⁶ A. SHALCHI,²⁸ H. SOL,¹⁰ D. SPANGLER,¹³ Ł. STAWARZ,²⁶ R. STEENKAMP,²⁹ C. STEGMANN,²¹ G. SUPERINA,¹⁶ P. H. TAM,⁶ J.-P. TAVERNET,²⁴ R. TERRIER,¹⁹ C. VAN ELDIK,² G. VASILEIADIS,²⁰ C. VENTER,¹⁴ J. P. VIALE,¹⁷ P. VINCENT,²⁴ M. VIVIER,¹² H. J. VÖLK,² F. VOLPE,¹⁶ S. J. WAGNER,⁶ M. WARD,¹³ AND A. A. ZDZIARSKI¹⁵

Received 2007 March 16; accepted 2007 June 5; published 2007 July 20

ABSTRACT

The high-frequency peaked BL Lac PKS 2155–304 at redshift $z = 0.116$ is a well-known VHE (>100 GeV) γ -ray emitter. Since 2002 its VHE flux has been monitored using the H.E.S.S. stereoscopic array of imaging atmospheric Cerenkov telescopes in Namibia. During the 2006 July dark period, the average VHE flux was measured to be more than 10 times typical values observed from the object. This article focuses solely on an extreme γ -ray outburst detected in the early hours of 2006 July 28 (MJD 53,944). The average flux observed during this outburst is $I(>200 \text{ GeV}) = (1.72 \pm 0.05_{\text{stat}} \pm 0.34_{\text{syst}}) \times 10^{-9} \text{ cm}^{-2} \text{ s}^{-1}$, corresponding to ~ 7 times the flux, $I(>200 \text{ GeV})$, observed from the Crab Nebula. Peak fluxes are measured with 1 minute timescale resolution at more than twice this average value. Variability is seen up to ~ 600 s in the Fourier power spectrum, and well-resolved bursts varying on timescales of ~ 200 s are observed. There are no strong indications for spectral variability within the data. Assuming the emission region has a size comparable to the Schwarzschild radius of a $\sim 10^9 M_{\odot}$ black hole, Doppler factors greater than 100 are required to accommodate the observed variability timescales.

Subject headings: BL Lacertae objects: individual (PKS 2155–304) — galaxies: active — gamma rays: observations

1. INTRODUCTION

Flux variability studies provide a strong probe into the physical processes of the innermost regions of active galactic nuclei (AGNs). Although the broadband emission from all AGNs is

highly variable, the most extreme flux variability, i.e., largest magnitude and shortest timescale, is observed from a class of

¹ Correspondence and request for material should be addressed to Wytan.Benbow@mpi-hd.mpg.de and Berrie.Giebels@poly.in2p3.fr.

² Max-Planck-Institut für Kernphysik, Heidelberg, Germany.

³ Dublin Institute for Advanced Studies, Ireland.

⁴ Yerevan Physics Institute, Armenia.

⁵ Centre d’Etude Spatiale des Rayonnements, CNRS/UPS, Toulouse, France.

⁶ Landessternwarte, Universität Heidelberg, Königstuhl, Germany.

⁷ Universität Hamburg, Institut für Experimentalphysik, Germany.

⁸ Now at CERN, Geneva, Switzerland.

⁹ Institut für Physik, Humboldt-Universität zu Berlin, Germany.

¹⁰ LUTH, UMR 8102 du CNRS, Observatoire de Paris, Section de Meudon, France.

¹¹ Laboratoire d’Astrophysique de Grenoble, INSU/CNRS, Université Joseph Fourier, Grenoble, France.

¹² DAPNIA/DSM/CEA, CE Saclay, Gif-sur-Yvette, France.

¹³ University of Durham, Department of Physics, UK.

¹⁴ Unit for Space Physics, North-West University, Potchefstroom, South Africa.

¹⁵ Nicolaus Copernicus Astronomical Center, Warsaw, Poland.

¹⁶ Laboratoire Leprince-Ringuet, Ecole Polytechnique, CNRS/IN2P3, Palaiseau, France.

¹⁷ Laboratoire d’Anecy-le-Vieux de Physique des Particules, CNRS/IN2P3, Anecy-le-Vieux, France.

¹⁸ European Associated Laboratory for Gamma-Ray Astronomy, jointly supported by CNRS and MPG.

¹⁹ APC, Paris, France.

²⁰ Laboratoire de Physique Théorique et Astroparticules, CNRS/IN2P3, Université Montpellier II, Montpellier, France.

²¹ Universität Erlangen-Nürnberg, Physikalisches Institut, Germany.

²² Now at University of Leeds, UK.

²³ Institut für Astronomie und Astrophysik, Universität Tübingen, Germany.

²⁴ LPNHE, IN2P3/CNRS, Universités Paris VI and VII, France.

²⁵ Institute of Particle and Nuclear Physics, Charles University, Prague, Czech Republic.

²⁶ Obserwatorium Astronomiczne, Uniwersytet Jagielloński, Kraków, Poland.

²⁷ Now at University of Adelaide, Australia.

²⁸ Institut für Theoretische Physik, Lehrstuhl IV: Weltraum und Astrophysik, Ruhr-Universität Bochum, Germany.

²⁹ University of Namibia, Windhoek, Namibia.

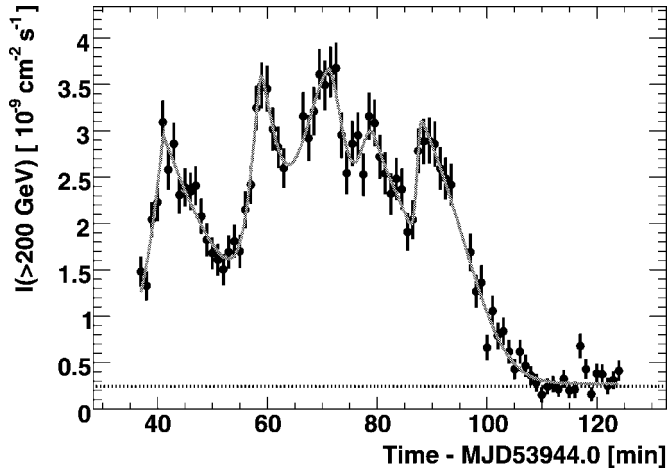


FIG. 1.—Integral flux above 200 GeV observed from PKS 2155–304 on MJD 53,944 vs. time. The data are binned in 1 minute intervals. The horizontal line represents $I(>200 \text{ GeV})$ observed (Aharonian et al. 2006) from the Crab Nebula. The curve is the fit to these data of the superposition of five bursts (see text) and a constant flux.

AGNs known as blazars. As a result, blazar variability studies are crucial to unraveling the mysteries of AGNs. Over a dozen blazars have been detected so far at very high energies (VHEs). In the southern hemisphere, PKS 2155–304 is generally the brightest blazar at these energies and is probably the best studied at all wavelengths. The VHE flux observed (Aharonian et al. 2005a) from PKS 2155–304 is typically of the order $\sim 15\%$ of the Crab Nebula flux above 200 GeV. The highest flux previously measured in one night is approximately 4 times this value, and clear VHE-flux variability has been observed on daily timescales. The most rapid flux variability measured for this source is 25 minutes (Aharonian et al. 2005b) occurring at X-ray energies. The fastest variation published from any blazar, at any wavelength, is an event lasting ~ 800 s, where the X-ray flux from Mrk 501 varied by 30% (Xue & Cui 2005),³⁰ while at VHEs doubling timescales as fast as ~ 15 minutes have been observed from Mrk 421 (Gaidos et al. 1996).

The High Energy Stereoscopic System (H.E.S.S.; Hinton 2004) is used to study VHE γ -ray emission from a wide variety of astrophysical objects. As part of the normal H.E.S.S. observation program, the flux from known VHE AGNs is monitored regularly to search for bright flares. During such flares, the unprecedented sensitivity of H.E.S.S. (5 standard deviation, σ , detection in ~ 30 s for a Crab Nebula flux source at 20° zenith angle) enables studies of VHE flux variability on timescales of a few tens of seconds. During the 2006 July dark period, the average VHE flux observed by H.E.S.S. from PKS 2155–304 was more than 10 times its typical value. In particular, an extremely bright flare of PKS 2155–304 was observed in the early hours of 2006 July 28 (MJD 53,944). This article focuses solely on this particular flare. The results from other H.E.S.S. observations of PKS 2155–304 from 2004 through 2006 will be published elsewhere.

2. RESULTS FROM MJD 53,944

A total of three observation runs (~ 28 minutes each) were taken on PKS 2155–304 in the early hours³¹ of MJD 53,944.

³⁰ Xue & Cui (2005) also demonstrate that a 60% X-ray flux increase in ~ 200 s observed (Catanese & Sambruna 2000) from Mrk 501 is likely an artifact.

³¹ The three runs began at 00:35, 01:06, and 01:36 UTC, respectively.

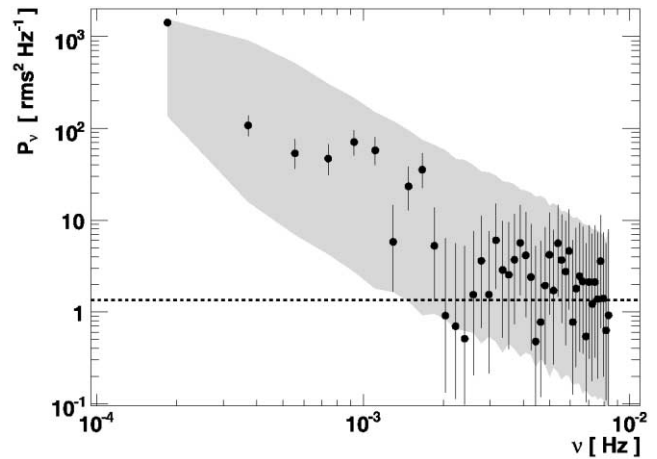


FIG. 2.—Fourier power spectrum of the light curve and associated measurement error. The gray shaded area corresponds to the 90% confidence interval for a light curve with a power-law Fourier spectrum $P_v \propto \nu^{-2}$. The horizontal line is the average noise level (see text).

These data entirely pass the standard H.E.S.S. data-quality selection criteria, yielding an exposure of 1.32 hr live time at a mean zenith angle of 13° . The standard H.E.S.S. calibration (Aharonian et al. 2004) and analysis tools (Benbow 2005) are used to extract the results shown here. As the observed signal is exceptionally strong, the event-selection criteria (Benbow 2005) are performed using the “loose cuts,” instead of the “standard cuts,” yielding an average postanalysis energy threshold of 170 GeV. The loose cuts are selected since they have a lower energy threshold and higher γ -ray and background acceptance. The higher acceptances avoid low-statistics issues by estimating the background and significance on short timescales, thus simplifying the analysis. The on-source data are taken from a circular region of radius $\theta_{\text{cut}} = 0.2^\circ$ centered on PKS 2155–304, and the background (off-source data) is estimated using the “Reflected-Region” method (Berge et al. 2007).

A total of 12,480 on-source events and 3296 off-source events are measured with an on-off normalization of 0.215. The observed excess is 11,771 events (~ 2.5 Hz), corresponding to a significance of 168σ calculated following the method of equation (17) in Li & Ma (1983). It should be noted that use of the standard cuts also yields a strong excess (6040 events, 159σ) and results (i.e., flux, spectrum, variability) consistent with those detailed later.

2.1. Flux Variability

The average integral flux above 200 GeV observed from PKS 2155–304 is $I(>200 \text{ GeV}) = (1.72 \pm 0.05_{\text{stat}} \pm 0.34_{\text{syst}}) \times 10^{-9} \text{ cm}^{-2} \text{ s}^{-1}$, equivalent to ~ 7 times the $I(>200 \text{ GeV})$ observed from the Crab Nebula (I_{Crab} ; Aharonian et al. 2006). Figure 1 shows $I(>200 \text{ GeV})$, binned in 1 minute intervals, versus time. The fluxes in this light curve range from $0.65 I_{\text{Crab}}$ to $15.1 I_{\text{Crab}}$, and their fractional rms variability amplitude (Vaughan et al. 2003) is $F_{\text{var}} = 0.58 \pm 0.03$. This is ~ 2 times higher than archival X-ray variability (Zhang et al. 1999, 2005). The Fourier power spectrum calculated from Figure 1 is shown in Figure 2. The error on the power spectrum is the 90% confidence interval estimated from 10^4 simulated light curves. These curves are generated by adding a random constant to each individual flux point, where this constant is taken randomly from a Gaussian distribution with a dispersion equal to the error of the respective point. The average power expected when the measurement error dominates is shown as a dashed line (see the Appendix in

Vaughan et al. 2003). There is power significantly above the measurement noise level up to 1.6×10^{-3} Hz (600 s). The power spectrum also shows that most of the power is at low frequencies. The gray shaded area shows the 90% confidence level obtained by simulating 10^4 light curves with a power-law Fourier spectrum $P_\nu \propto \nu^{-2}$ (Timmer & Koenig 1995) and a random Gaussian error as above. The power spectrum derived from the data is thus compatible with a light curve generated by a stochastic process with a power-law Fourier spectrum of index -2 . An index of -1 produces too much power at high frequencies and is rejected. These power spectra are remarkably similar to those derived in X-rays (Zhang et al. 1999) from the same source.

Rapid variability is clearly visible in substructures that appear in the light curve, with even shorter rise and decay timescales than those found in the Fourier analysis. In order to quantify those timescales, the light curve is considered to be consisting of a series of bursts, which is common for AGNs and γ -ray bursts (GRBs). The “generalized Gaussian” shape from Norris et al. (1996) is used to characterize these bursts, where the burst intensity is described by $I(t) = A \exp[-(|t - t_{\max}|/\sigma_{r,d})^\kappa]$, where t_{\max} is the time of the burst’s maximum intensity (A); σ_r and σ_d are the rise ($t < t_{\max}$) and decay ($t > t_{\max}$) time constants, respectively; and κ is a measure of the burst’s sharpness. The rise and decay times, from half to maximum amplitude, are $\tau_{r,d} = (\ln 2)^{1/\kappa} \sigma_{r,d}$. A peak finding tool, using a Markov chain algorithm (Morhac et al. 2000), selected five significant bursts. A function consisting of a superposition of an identical number of bursts plus a constant signal was fit³² to the data. The best fit has a χ^2 probability of 20%, and the fit parameters are shown in Table 1. Interestingly, there is a marginal trend for κ to increase with subsequent bursts, making them less sharp, as the flare progresses. The κ values are close to the bulk of those found by Norris et al. (1996), but the timescales measured here are 2 orders of magnitude larger.

During both the first two bursts, there is clear doubling of the flux within τ_r . Such doubling is sometimes used as a characteristic timescale of flux variability. For compatibility with such estimators, the definition of doubling time, $T_2 =$

³² The Markov chain burst positions were used to initialize t_{\max} for each burst. All parameters are left free in the fit.

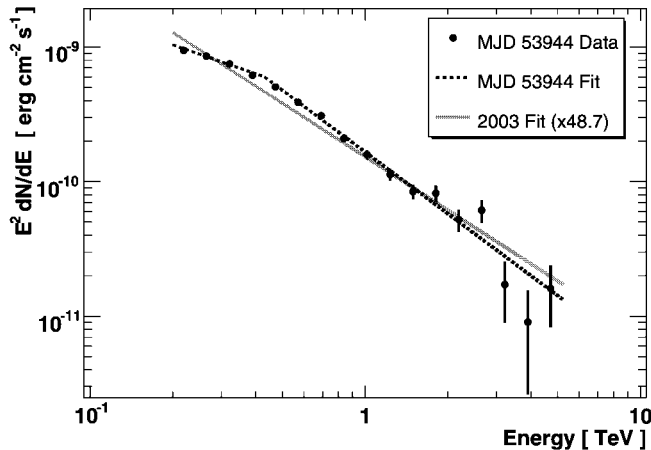


FIG. 3.—Time-averaged spectrum observed from PKS 2155–304 on MJD 53,944. The dashed line is the best χ^2 fit of a broken power law to the data. The solid line represents the fit to the time-averaged spectrum of PKS 2155–304 from 2003 (Aharonian et al. 2005a) scaled by 48.7. Neither spectrum is corrected (see, e.g., Aharonian et al. 2005b) for the absorption of VHE γ -rays on the extragalactic background light.

$|I_{ij}\Delta T/\Delta I|$, from Zhang et al. (1999) was used.³³ Here $\Delta T = T_j - T_i$, $\Delta I = I_j - I_i$, $I_{ij} = (I_j + I_i)/2$, with T and I being the time and flux, respectively, of any pair of points in the light curve. The fastest $T_2 = 224 \pm 60$ s is compatible with the fastest significant timescale found by the Fourier transform. Averaging the five lowest T_2 values yields 330 ± 40 s.

The variability timescales of these bursts are among (see also Albert et al. 2007) the fastest ever seen in a blazar, at any wavelength, and are almost an order of magnitude smaller than those previously observed from this object. It should be noted that similar timescales are found with even smaller binning (e.g., 20 s) of the H.E.S.S. light curve and that many checks of the data quality were undertaken to ensure that the flux variations cannot be the result of background fluctuations, atmospheric events, etc. In addition, all the results have been verified using an independent calibration method and alternative analysis techniques.

2.2. Spectral Analysis

Figure 3 shows the time-averaged photon spectrum for these data. The data are well fit, $\chi^2 = 17.1$ for 13 degrees of freedom (dof), by a broken power-law function:

$$E < E_B : \frac{dN}{dE} = I_0 \left(\frac{E}{1 \text{ TeV}} \right)^{-\Gamma_1},$$

$$E > E_B : \frac{dN}{dE} = I_0 \left(\frac{E_B}{1 \text{ TeV}} \right)^{(\Gamma_2 - \Gamma_1)} \left(\frac{E}{1 \text{ TeV}} \right)^{-\Gamma_2},$$

where $I_0 = (2.06 \pm 0.16 \pm 0.41) \times 10^{-10} \text{ cm}^{-2} \text{ s}^{-1} \text{ TeV}^{-1}$, $E = 430 \pm 22 \pm 80 \text{ GeV}$, $\Gamma_1 = 2.71 \pm 0.06 \pm 0.10$, and $\Gamma_2 = 3.53 \pm 0.05 \pm 0.10$. For each parameter, the two uncertainties are the statistical and systematic values, respectively. Fits to the data of either a simple power law ($\Gamma = 3.19 \pm 0.02 \pm 0.10$, $\chi^2 = 138$, 15 dof) or a power law with an exponential cutoff ($\chi^2 = 45$, 14 dof) are not acceptable. The time-averaged spectrum ($\Gamma = 3.32$) of PKS 2155–304 measured in 2003 (Aharonian et al. 2005a) multiplied by the ratio (48.7) of $I(>200 \text{ GeV})$ from the respective data sets, is also shown in Figure 3. Despite a factor of ~ 50 change in flux, there is qualitatively little difference between the two spectra. Indeed, fitting a broken power law to the current data set, keeping Γ_1 and Γ_2 fixed to the values measured in 2003, yields a value for E_B consistent with that measured in 2003. The small difference is surprising since a change of the spectral shape with varying flux levels, typically hardening with increased flux, has often been observed from blazars at X-ray energies (see, e.g., Giommi et al. 1990), as well as in the VHE domain (see, e.g., Aharonian et al. 2002).

³³ Only values of T_2 with less than 30% uncertainty are considered.

TABLE 1
RESULTS OF THE BEST χ^2 FIT OF THE SUPERPOSITION OF FIVE BURSTS AND A CONSTANT TO THE DATA SHOWN IN FIGURE 1

t_{\max} (minutes)	A ($10^{-9} \text{ cm}^{-2} \text{ s}^{-1}$)	τ_r (s)	τ_d (s)	κ
41.0	2.7 ± 0.2	173 ± 28	610 ± 129	1.07 ± 0.20
58.8	2.1 ± 0.9	116 ± 53	178 ± 146	1.43 ± 0.83
71.3	3.1 ± 0.3	404 ± 219	269 ± 158	1.59 ± 0.42
79.5	2.0 ± 0.8	178 ± 55	657 ± 268	2.01 ± 0.87
88.3	1.5 ± 0.5	67 ± 44	620 ± 75	2.44 ± 0.41

NOTE.—The constant term is $(0.27 \pm 0.03) \times 10^{-9} \text{ cm}^{-2} \text{ s}^{-1}$ ($1.1I_{\text{Crab}}$).

The high flux observed from PKS 2155–304 allows the determination of accurate photon spectra on timescales of the order of minutes. Therefore, a simple search for temporal changes of the VHE spectral shape within these data was performed. Spectra were determined for consecutive data slices of 28 minutes (1 run), 10 minutes, and 5 minutes. Fitting the time-average spectral shape, allowing only the normalization (I_0) to vary, to these short-timescale spectra yields reasonable χ^2 probabilities. Thus, there are no strong indications of fast spectral variability. However, weak variations ($\Delta\Gamma < 0.2$) are not ruled out. A more sophisticated study of any fast spectral variations within these data is beyond the scope of this Letter and will be published elsewhere.

3. DISCUSSION

It is very likely that the electromagnetic emission in blazars is generated in jets that are beamed and Doppler-boosted toward the observer. Superluminal expansions observed with VLBI (Piner & Edwards 2004) provide evidence for moderate Doppler boosting in PKS 2155–304. Causality implies that γ -ray variability on a timescale t_{var} , with a Doppler factor³⁴ (δ), is related to the radius (R) of the emission zone by $R \leq ct_{\text{var}}\delta/(1+z)$. Conservatively using the best-determined rise time (i.e., τ , with the smallest error) from Table 1 for $t_{\text{var}} = 173 \pm 28$ s (note that this is similar to the fastest T_2) limits the size of the emission region to $R\delta^{-1} \leq 4.65 \times 10^{12}$ cm ≤ 0.31 AU.

The jets of blazars are believed to be powered by accretion onto a supermassive black hole (SMBH). Thus, accretion/ejection properties are usually presumed to scale with the Schwarzschild radius R_s of the SMBH, where $R_s = 2GM/c^2$, which is the smallest, most-natural size of the system (see, e.g., Blandford & Payne 1982). Expressing the size R of the γ -ray-emitting region in terms of R_s , the variability timescale limits its mass by $M \leq [c^3 t_{\text{var}} \delta / 2G(1+z)] R_s / R \sim 1.6 \times 10^7 M_\odot \delta R_s / R$. The reported³⁵ host galaxy luminosity $M_R = -24.4$ (Kotilainen et al. 1998, Table 3) would imply a SMBH mass of order $(1-2) \times 10^9 M_\odot$ (Bettoni et al. 2003) and therefore $\delta \geq (60-120) R/R_s$. Emission regions of only a few R_s would require values of δ much greater than those typically derived for blazars ($\delta \sim 10$) and come close

³⁴ With δ defined in the standard way as $[\Gamma(1 - \beta \cos \theta)]^{-1}$, where Γ is the bulk Lorentz factor of the plasma in the jet, $\beta = v/c$, and θ is the angle to the line of sight.

³⁵ See Wurtz et al. (1996) and $M_R > -23.1$ (for $h = 0.5$) showing the need for confirmation of this value.

to those used for GRBs, which would be a challenge to understand. For example, the subparsec VHE γ -ray-emitting plasma would have to decelerate with a high efficiency to accommodate relatively small Lorentz factors observed at parsec scales (Piner & Edwards 2004). It is possible, however, that the SMBH mass is overestimated, reducing the δ constraint by the same factor, or that the variability has an origin (e.g., a geometric effect from jet bending as discussed in Wagner et al. 1993) unrelated to the black hole. Detailed modeling of the spectral energy distribution of PKS 2155–304, during the multiple VHE flares observed by H.E.S.S. in the 2006 July dark period, including simultaneous multifrequency data, will appear elsewhere.

The VHE variability observed in this particular flaring episode is the fastest ever observed from a blazar. While the variability is a factor of 5 times faster than that previously measured from Mrk 421 (Gaidos et al. 1996) in terms of the light-crossing time of the Schwarzschild radius, R_s/c , the variability of PKS 2155–304 is another factor of $\approx 6-12$ more constraining assuming a $10^{8.22} M_\odot$ for Mrk 421 (Woo et al. 2005). It should also be noted that the choice of a ~ 3 minute variability timescale here is conservative and that the light curve is strongly oversampled, allowing for the first time in the VHE regime a detailed statistical analysis of a flare, which shows remarkable similarity to other longer duration events at X-ray energies. From such rapid variability one must conclude that either very large Doppler factors can be present in AGN jets, or that the observed variability is not connected to the central black hole, clearly showing the power of Cerenkov-telescope arrays in probing the internal mechanisms in BL Lac objects.

The support of the Namibian authorities and of the University of Namibia in facilitating the construction and operation of H.E.S.S. is gratefully acknowledged, as is the support by the German Ministry for Education and Research (BMBF), the Max Planck Society, the French Ministry for Research, the CNRS-IN2P3, and the Astroparticle Interdisciplinary Programme of the CNRS, the UK Particle Physics and Astronomy Research Council (PPARC), the IPNP of the Charles University, the Polish Ministry of Science and Higher Education, the South African Department of Science and Technology and National Research Foundation, and by the University of Namibia. We appreciate the excellent work of the technical support staff in Berlin, Durham, Hamburg, Heidelberg, Palaiseau, Paris, Saclay, and in Namibia in the construction and operation of the equipment.

REFERENCES

- Aharonian, F., et al. 2002, *A&A*, 393, 89
 ———. 2004, *Astropart. Phys.*, 22, 109
 ———. 2005a, *A&A*, 430, 865
 ———. 2005b, *A&A*, 442, 895
 ———. 2006, *A&A*, 457, 899
 Albert, J., et al. 2007, *ApJ*, in press (astro-ph/0702008)
 Benbow, W. 2005, in *Towards a Network of Atmospheric Cherenkov Detectors VII*, ed. B. Degrange & G. Fontaine (Palaiseau: Ecole Polytechnique), 163
 Berge, D., Funk, S., & Hinton, J. 2007, *A&A*, 466, 1219
 Bettoni, D., Falomo, R., Fiasano, G., & Govoni, F. 2003, *A&A*, 399, 869
 Blandford, R. D., & Payne, D. G. 1982, *MNRAS*, 199, 883
 Catanese, M., & Sambruna, R. M. 2000, *ApJ*, 534, L39
 Gaidos, J. A., et al. 1996, *Nature*, 383, 319
 Giommi, P., et al. 1990, *ApJ*, 356, 432
 Hinton, J. 2004, *NewA Rev.*, 48, 331
 Kotilainen, J. K., Falomo, R., & Scarpa, R. 1998, *A&A*, 336, 479
 Li, T., & Ma, Y. 1983, *ApJ*, 272, 317
 Morhac, M., et al. 2000, *Nucl. Instrum. and Methods Phys. Res. A*, 443, 108
 Norris, J. P., et al. 1996, *ApJ*, 459, 393
 Piner, B. G., & Edwards, P. G. 2004, *ApJ*, 600, 115
 Timmer, J., & Koenig, M. 1995, *A&A*, 300, 707
 Vaughan, S., Edelson, R., Warwick, R. S., & Uttley, P. 2003, *MNRAS*, 345, 1271
 Wagner, S. J., et al. 1993, *A&A*, 271, 344
 Woo, J.-H., et al. 2005, *ApJ*, 631, 762
 Wurtz, R., Stocke, J. T., & Yee, H. K. C. 1996, *ApJS*, 103, 109
 Xue, Y., & Cui, W. 2005, *ApJ*, 622, 160
 Zhang, Y. H., et al. 1999, *ApJ*, 527, 719
 ———. 2005, *ApJ*, 629, 686